Biochimica et Biophysica Acta 820 (1985) 305–314
Elsevier

BBA 72799

Determination of intracellular conductivity from electrical breakdown measurements

G. Pilwat [a] and U. Zimmermann [b,*]

[a] *Arbeitsgruppe Membranforschung am Institut für Medizin, Kernforschungsanlage Jülich GmbH, Postfach 1913, D-5170 Jülich and* [b] *Lehrstuhl für Biotechnologie, Universität Würzburg, Röntgenring 11, D-8700 Würzburg (F.R.G.)*

(Received May 6th, 1985)

Key words: Intracellular conductivity; Electrical breakdown

The intracellular resistivity (conductivity) of cells can be easily calculated with high accuracy from electrical membrane breakdown measurements. The method is based on the determination of the size distribution of a cell suspension as a function of the electrical field strength in the orifice of a particle volume analyser (Coulter counter). The underestimation of the size distribution observed beyond the critical external field strength leading to membrane breakdown represents a direct access to the intracellular resistivity as shown by the theoretical analysis of the data. The potential and the accuracy of the method is demonstrated for red blood cells and for ghost cells prepared by electrical haemolysis. The average value of 180 Ω · cm for the intracellular resistivity of intact red blood cells is consistent with the literature.

Introduction

There is an extensive bulk of literature covering the field of reversible electrical breakdown of cell membranes [1–5] and artificial bilayer membranes [6–10]. The possibility of efficiently carrying out genetic manipulation and fusion of cells (electrofusion, magneto-electrofusion and electro-acoustic fusion) by means of electrical breakdown has considerably stimulated further research on high electric field effects on biological and artificial membranes in recent years [4,5,11–16].

In this communication we will be considering a new application of the electrical breakdown technique, namely the determination of intracellular conductivity of cells. The possibility of measuring this parameter by way of electrical breakdown measurements was already pointed out by us at an early stage [17,18] and later confirmed by Akeson and Mel [19,20]. However, at that time the necessary equipment was too sophisticated or else the measurements were too time-consuming.

In this paper we shall demonstrate that this interesting parameter can be determined relatively quickly and easily by measuring the size distribution of a cell suspension as a function of the electric-field strength in the orifice of a particle volume analyser. Above a critical field strength which gives rise to electrical breakdown of the membrane, the distribution is underestimated. The extent of this underestimation enables direct determination of the internal conductivity of the cell. The necessary analysers (also known as Coulter counters) are available in almost every (clinical) laboratory, so that, generally speaking, measurements of this kind require no new apparatus.

Theoretical considerations

In order to determine the intracellular conductivity from reversible electrical breakdown mea-

* To whom reprint requests should be addressed.

surements and to perform the associated measurement of virtual volume after electrical breakdown, it is necessary to consider in detail the fundamental equations for the treatment of the problem in question. The aim is then to demonstrate how the cell-dependent signals before and after reversible electrical breakdown can be related to the intracellular conductivity with the aid of these systems of equations.

According to Velick and Gorin [21], the conductivity, k, of a suspension of cells with an ellipsoid shape is determined by the following equation:

$$k = k_1 - \frac{2kr}{1-r}\left(\frac{1}{2 - abcL_a}\right) \tag{1}$$

k, k_1 and k_2 are the conductivities of the suspension, medium and cells, respectively. r is the fraction of the total volume occupied by the suspended cells. a, b and c represent the three axes of the cell, and L_a is an elliptical integral.

Eqn. 1 presupposes that the suspended cells can be regarded as nonconductive (i.e. that their specific conductivity, k_2, is equal to zero) and that the external electrical field is applied parallel to the longitudinal axis of the cell. Because of the high membrane resistance, the first condition is always fulfilled for virtually all cell types. The second condition is also fulfilled in the experiments described here, because hydrodynamic focussing aligns the cells in such a way that their longitudinal axis is parallel to the field (and to the direction of the current) [1].

Substituting the conductivities by the corresponding resistivities and solving Eqn. 1 for r provides the following equation

$$r = \frac{(\rho/\rho_1) - 1}{(\rho/\rho_1) - 1 + f_1} \tag{2}$$

ρ, ρ_1 and ρ_2 are the electrical resistivities of the suspension, medium and cells, respectively. f_1 represents the so-called shape factor which takes into consideration the different axial ratios of the ellipsoid. f_1 is defined by the following equation:

$$f_1 = \frac{2}{2 - abcL_a} \tag{3}$$

Let us now consider a prolate ellipsoid of revolution in the orifice of a particle analyser. The ratio of the volume of the particle (cell), v_p, to the volume of the orifice, v_o, is $r = v_p/v_o$. The resistance R of the orifice with a suspended particle is $R = R_1 + \Delta R_1$, where R_1 is the resistance of the orifice without particle and ΔR_1 is the resistance change of the orifice caused by a particle. Written in terms of the resistivities,

$$\rho = \rho_1 + \Delta R_1 \cdot A/L \tag{4}$$

where A is the area and L the effective length of the orifice, we introduce these parameters into Eqn. 2 and obtain:

$$\frac{v_p}{v_o} = \frac{\Delta R_1/R_1}{\Delta R_1/R_1 + f_1} \tag{5}$$

Solving Eqn. 5 for the relative resistance change provides the following equation:

$$\frac{\Delta R_1}{R_1} = \frac{v_p}{v_o} \cdot \left(f_1 + \frac{\Delta R_1}{R_1}\right) \tag{6}$$

If we assume that the change in orifice resistance, ΔR_1, is small in relation to the resistance of the orifice, R_1, i.e. that $\Delta R_1 \ll R_1$, it follows that $\Delta R_1/R \ll f_1$ must also be valid:

$$\frac{\Delta R_1}{R_1} = \frac{v_p}{v_o} \cdot f_1 \tag{7}$$

Eqn. 7 represents a well-known relationship, namely that the relative change in resistance elicited by the presence of a particle in the orifice of a particle volume analyser is proportional to the volume of the particle [22,23]. We have already pointed out that this relationship is only valid for electrically non-conducting particles.

In the case of electrically conducting particles, e.g. cells which have undergone electrical breakdown of the cell membrane in the presence of sufficiently high external fields in the orifice, the following equation for the conductivity of a suspension of cells applies instead of Eqn. 1 (the symbols retain their meaning) [21]:

$$k = k_1 + \left(\frac{r}{1-r}\right)\left(\frac{2(k_2 - k)}{2 + abcL_a[(k_2/k_1) - 1]}\right) \tag{8}$$

Eqn. 8 is also based on the condition that the electric field is applied parallel to the longitudinal axis of the cell. If this equation is again solved for r and the conductivities are substituted by the corresponding resistivities, the following equation is obtained:

$$r = \frac{(\rho/\rho_1)-1}{(\rho/\rho_1)-1+\frac{2[1-(\rho/\rho_2)]}{2+abcL_a[(\rho_1/\rho_2)-1]}} \quad (9)$$

The treatment of electrically conducting cells in the orifice of a particle volume analyser is based on the same preconditions as the derivation of Eqn. 5, so that the following equation can be derived in analogy to Eqn. 6:

$$\frac{\Delta R_1}{R_1} = \frac{v_p}{v_o}\left(\frac{\Delta R_1}{R_1}+\frac{2[1-(\rho_1+\Delta R_1 \cdot A/L)/\rho_2]}{2+abcL_a[(\rho_1/\rho_2)-1]}\right) \quad (10)$$

In analogy with Eqn. 7, the assumption that $\Delta R_1 \ll R_1$ yields the following:

$$\frac{\Delta R_1}{R_1} = \frac{v_p}{v_o} \cdot f_2 \quad (11)$$

where f_2 is defined by the following equation:

$$f_2 = \frac{2[1-(\rho_1/\rho_2)]}{2+abcL_a[(\rho_1/\rho_2)-1]} \quad (12)$$

The shape factor f_2 takes into account both the axial ratios and the ratio of the resistivities of particles and medium. Apart from the shape factors, Eqns. 7 and 11 are thus identical. The relationship given by Eqn. 12 was first derived by Kachel [24]. Eqns. 7 and 11 represent the key equations for the determination of the intracellular conductivities of cells. A comparison of the terms $v_p f_1$ (size measurement in the non-conducting state, i.e. prior to electrical breakdown) and $v_p f_2$ (size measurement in the conducting state, i.e. post-breakdown conditions) should therefore provide the specific internal resistance of the cells if the specific resistance of the medium is known. Under experimental conditions (see below), this involves measuring the slope of the signal versus electric field strength (or current in the orifice) curves before and after breakdown.

Experimental analysis

We have shown that Eqns. 7 and 11 are generally valid for the relative resistance change of a cell in the orifice of a particle volume analyser. The preamplifier of choice for resistance pulse sizing is the current-sensing amplifier. A particle in the orifice will cause this amplifier to produce an output voltage of (see Ref. 25):

$$\Delta V = \frac{f v_p}{v_o} \cdot R_f \cdot i \quad (13)$$

where i is the current through the orifice and R_f is the feedback resistance of the preamplifier.

If the mean pulse height, ΔV, of a cell size distribution is plotted against the current, i, through the orifice, a straight line is obtained in accordance with Ohm's law (see Fig. 1). The straight line changes its slope at the characteristic current intensity (or field strength) at which electrical breakdown of the cell membrane occurs. Above this characteristic current value, current is able to flow partly through the cell interior, so that the signal, ΔV, is reduced. Before breakdown, the slope of the signal versus current curve is proportional to the volume (see Eqn. 7). After breakdown, the slope of the straight line is determined by the ratio of the internal conductivity of the cell to that of the medium. If the conductivity of the cell is higher after breakdown that that of the medium, the slope may become negative (Ref. 26, see also below). If the slope is zero, i.e. if the signal ΔV remains constant with increasing current, i, then the resistivity of the cell interior equals that of the medium. The two straight lines can therefore be described by the following mathematical expressions:

(1) Pre-breakdown

$$\Delta V_1 = \frac{f_1 v_{p1}}{v_o} \cdot R_f \cdot i \quad (14)$$

(2) Post-breakdown

$$\Delta V_2 = \frac{f_2 \cdot v_{p2}}{v_o} \cdot R_f \cdot i + \Delta V_o \quad (15)$$

Since the electrically effective volume v_o and the resistance R_f are constant and the volume v_{p2} of

the electrically conducting cell is equal to the volume, v_{p1}, of the non-conducting cell, the ratio of the slopes, s, yields:

$$s = \frac{f_2}{f_1} \tag{16}$$

i.e. the two shape factors are in the same ratio as the slopes of the two straight lines. If f_1 and f_2 are substituted by Eqns. 3 and 12, respectively, we obtain:

$$s = \frac{[1-(\rho_1/\rho_2)](2-abcL_a)}{2+abcL_a[(\rho_1/\rho_2)-1]} \tag{17}$$

Solving this equation for the internal resistivity ρ_2 and substituting the term $abcL_a$ in this equation by $2-(2/f_1)$ [21], where f_1 is the shape factor of an ellipsoid with its longitudinal axis aligned in parallel with the direction fo the field, provides the equation for the resistivity of the cell.

$$\rho_2 = \rho_1\left(\frac{s \cdot f_1}{1-s}+1\right) \tag{18}$$

This key equation shows that for any given resistivity of the suspension medium, the internal resistivity (or the internal conductivity) of a cell can be calculated from the ratio of the slopes after and before breakdown (Fig. 1).

Methods

Sample preparation. Human blood was withdrawn from apparently healthy donors and was stored in acid/citrate/dextrose buffer. The experiments were performed on the same day.

Haemoglobin determination. The haemoglobin determination was performed using the cyanmethaemoglobin method of Sigma Chemicals Co. (Diagnostic Kit No. 525). The resulting blood haemoglobin values in gm/100 ml were related to the erythrocyte concentration of the blood yielding the haemoglobin content in pg per erythrocyte.

Spherical shape. Erythrocytes of spherical shape were prepared by the procedure of Haest et al. [27]. For this purpose the erythrocytes were incubated for 20 min in 0.95% NaCl solution containing 75 μg/ml Triton X-100. The transformation from the biconcave shape into the spherical shape was inspected under the microscope.

Ghost cell preparation. Ghost cells were prepared by electrically induced haemolysis [28] (see also Ref. 29). Briefly, red blood cells were washed and incubated in a solution (sodium phosphate-buffered KCl solution), pH 7, of the following composition (in mM): KCl, 105; NaCl, 20; $MgCl_2$, 4; Na_2HPO_4, 7.6; NaH_2PO_4, 2.4; and glucose, 10. The suspension density was 1 : 10 (packed cells to solution). An exponentially decaying field is applied to the cell suspension by discharging a capacitor using a spark gap. The electric field strength was 10 kV/cm and the pulse duration (decay time constant) was 40 μs. The temperature of the suspension was kept at 4°C. Haemolysis and equilibration with the external solution occurs in about 5 min. For resealing of the cells after 10 min the temperature was raised to 37°C for 30 min. After resealing, the cells were centrifugated at $10000 \times g$ for 10 min. For electrical haemolysis in hypotonic medium the isotonic medium was diluted with distilled water in the ratio of 3 : 1 (medium to water).

Measurement of size distribution. The size distribution of the red blood cells and the red blood cell ghosts were measured with a hydrodynamically focussing Coulter counter (Modell TF) [1,30]. The cells were incubated in isotonic NaCl solutions with different conductivities. The various conductivities (or resistances) of the medium were obtained by adding increasing amounts of isotonic sucrose solution to an isotonic NaCl solution. The size distributions were measured at increasing current through the orifice (field strength) of the Coulter counter (orifice dimensions: 60 μm in length and diameter). The resistivity of the sheath flow was always adapted to that of the medium in which the cells were suspended.

Results

In order to test Eqn. 18, size distributions of red blood cells were measured as a function of the current through the orifice and the mean pulse heights plotted versus the current. The conductivity of the medium was changed for each experimental run. If Eqn. 18 is valid, we can expect the value of the internal conductivity to be independent of the external conductivity (because the

membrane is practically impermeable and the period of measurement is relatively short, so that there should be no change in the internal ion composition). The result of a typical experimental run is shown in Fig. 1A. It is evident that beyond the point of breakdown, the slope of the straight line decreases with increasing sucrose concentration and the associated increase in resistance; in other words, the extracellular conductivity progressively approaches the conductivity of the cell interior.

Fig. 1A also shows that as the resistance of the solution increases, the current value at which breakdown occurs is reduced. This is to be expected on the basis of Ohm's law, assuming that the addition of sucrose does not change the breakdown voltage. This assumption can be confirmed by plotting the electric-field strength as the variable parameter instead of the current (see Fig. 1B). The critical field strength is independent of the conductivity of the solution, and so is the electrical breakdown voltage, according to the integrated Laplace equation [26].

The calculation of ρ_2 on the basis of Eqn. 18 and the experimental data of Fig. 1 are shown in Table I. The shape factor had a value of 1.09 which was calculated from the ratio of the axes of red blood cells [22] taken from photographs using the method of Kachel [31]. As expected, the specific resistance of the cell interior is constant within the limits of accuracy of measurement of 1%. This is further confirmed in Fig. 2 where the reciprocal value of the term $[s \cdot f_1/(1-s)]+1$ has been plotted against the specific resistance of the medium. The measured points all lie on a straight line which passes through zero in accordance with the theory.

Extrapolation of the straight line to the value $([s \cdot f_1/(1-s)]+1)^{-1} = 1$ provides the specific resistance of the external solution which matches the specific resistance of the cell interior.

In the case of the experiment represented in Figs. 1 and 2 and Table I, the specific resistance of the cell is 190 $\Omega \cdot$ cm. Measurements carried out on 49 different blood samples gave values between 140 $\Omega \cdot$ cm and 220 $\Omega \cdot$ cm.

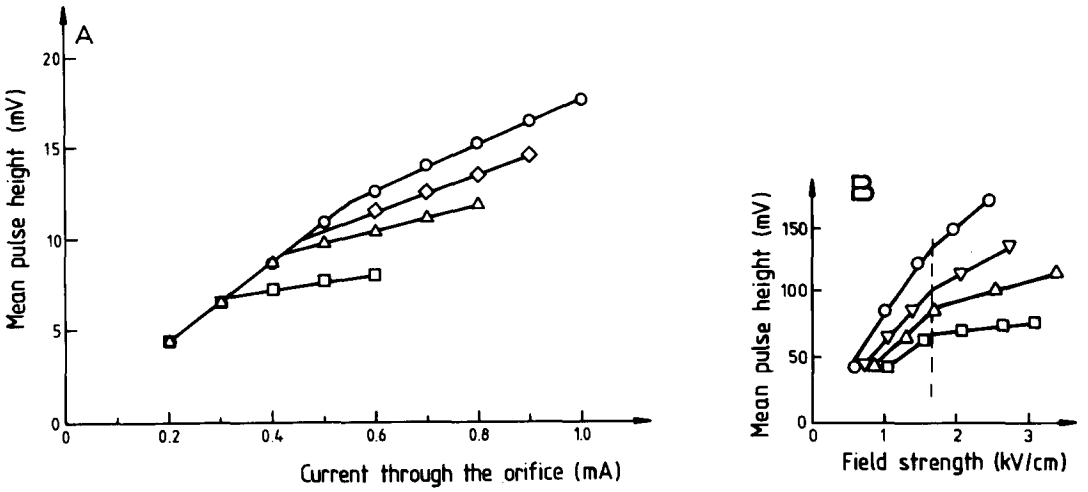

Fig. 1. The effect of increasing resistivity of the suspension medium on the pulse height of size distributions of human red blood cells measured as a function of the current through the orifice of a particle volume analyser. The different resistivities were achieved by adding isotonic sucrose solution to an isotonic NaCl solution. Resistivities and final sucrose concentrations: ○———○, 69.4 $\Omega \cdot$cm, 0 mM; ◇———◇ (A) and ▽———▽ (B), 98.6 $\Omega \cdot$cm, 90 mM; △———△, 120 $\Omega \cdot$cm, 120 mM; □———□, 145.5 $\Omega \cdot$cm, 150 mM. Before electrical breakdown for a given current the mean pulse heights of the size distributions are independent of the resistivity of the suspension medium. This is because the analyser uses a 'current-sensing' amplifier. After electrical breakdown the mean pulse heights of the size distributions depend on the resistivity of the medium. With increasing resistivities of the medium and therefore higher resistances in the orifice the electrical breakdown occurs at smaller currents. Nevertheless, the electrical field strength for breakdown is constant for all resistivities of the incubation medium as demonstrated in (B).

TABLE I

INTRACELLULAR RESISTIVITY OF RED BLOOD CELLS CALCULATED ACCORDING TO EQN. 18

The ratios of the slopes were obtained from measurements of the mean pulse height of a red blood cell population versus the orifice current. The different resistivities were achieved by adding isotonic sucrose solution to an isotonic NaCl solution (Measurements partly shown in Fig. 1).

Sucrose concn. (mM)	Resistivity of the medium, ρ_1 ($\Omega \cdot$cm)	Ratio of slopes, s	Intracellular resistivity, ρ_2 ($\Omega \cdot$cm)
0	69.4	0.61	187.7
30	77.5	0.57	189.5
60	87.0	0.53	190.9
90	98.6	0.46	190.2
120	120.0	0.35	190.4
150	145.5	0.21	187.6

It was necessary to test whether this variation is attributable to variations in the haemoglobin content. It is evident from Fig. 3 that no correlation between the mean haemoglobin content (related to pg haemoglobin per erythrocyte) and the intracellular resistance can be found. We were unable to elucidate the cause of these variations in the internal specific resistance of red blood cells, but they must be attributable to different ion concentrations. It is worth mentioning, in this context, that the variation in the resistance values agrees with the results of Pauly and Schwan [32].

In the experiments described above, a flow velocity was chosen which led to maximum deformation. Maximum deformation leads to an axial ratio of 3.75 which corresponds to a shape factor of 1.09. To test whether the measurement of the intracellular specific resistance might be dependent on the shape, that is on the deformation of the cells in the hydrodynamically focussing measurement orifice, spherical cells (shape factor 1.5) were investigated and compared with prolate ellipsoids (shape factor 1.09). The spherical shape was induced with Triton X-100 (see Methods). In spite of the different axial ratios and associated shape factors, the same specific resistances were measured for the cell interior.

In the following set of experiments the validity of Eqn. 18 was tested on ghost cells because these cells allow the internal conductivity to be changed in a controlled manner and because any influence exerted by haemoglobin can be largely eliminated. Ghost cells were obtained by electrical haemolysis in isotonic sodium phosphate-buffered KCl solution (see Methods). This solution was taken up by the cells during the resealing process at 37°C, and had a specific resistance of 63.0 $\Omega \cdot$ cm. Since haemolysis was carried out at a 1 : 10 ratio of red blood cells to medium, 10% of the haemoglobin remained in the cells [33]. In analogy to the experiments on intact red blood cells, signal versus current curves were determined for media of different conductivities. Fig. 4 shows that after electrical breakdown, the signal, ΔV, of the ghost cells also decreases with increasing current. Since most of the haemoglobin has been removed, the cell inter-

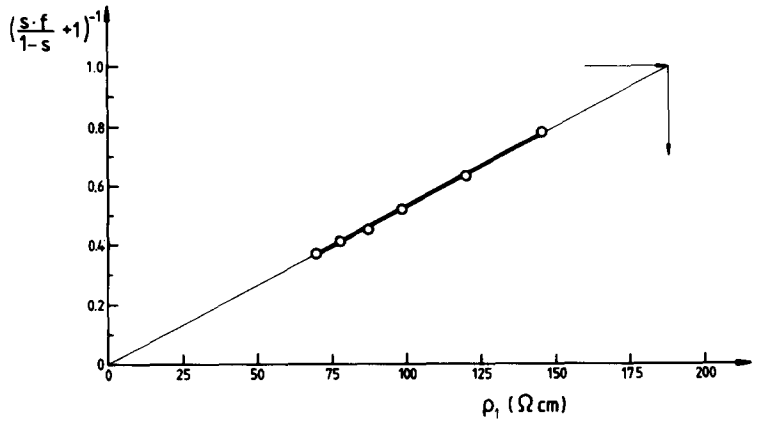

Fig. 2. The relationship of the reciprocal value of the term $[s \cdot f/(1-s)]+1$ in Eqn. 18 to the resistivity of the medium, ρ_1 for the data presented in Table I. The resulting straight line can be extrapolated for $([s \cdot f/(1-s)]+1)^{-1}=1$ leading to a value for the resistivity of the cell interior. The result indicates that the measurement of the intracellular resistance can be conducted at any extracellular resistance.

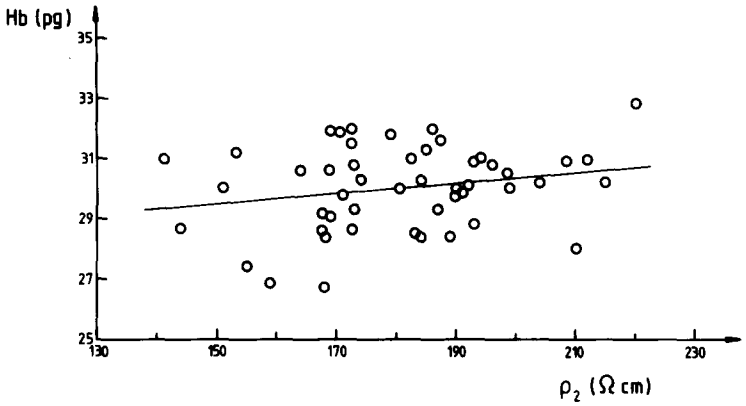

Fig. 3. The intracellular haemoglobin content of human red blood cells versus the intracellular resistivity, ρ_2. The graph represents 49 blood samples. There is obviously no correlation between the haemoglobin content and the intracellular resistivity. Mean value for haemoglobin content: (30.1 + 1.4) pg, mean value for the resistivity: (180 + 18) $\Omega \cdot$cm.

ior becomes more conductive than the external medium at sucrose concentrations as low as 35 mM, so that the slope assumes negative values after breakdown. The calculation of the internal specific resistance from the curves in Fig. 4 using Eqn. 18 is shown in Table II. Because the cells were found to be spherical when inspected under the microscope and because the flow velocities used in the experiment should not have deformed them, the shape factor was taken to be 1.5. Table II shows that the calculated internal specific resistance is constant within the error limits of 5% and independent of the conductivity of the external medium. When the values are plotted as in Fig. 2, the same value is obtained. With 69 $\Omega \cdot$ cm, the resistivity of the interior of the ghost cells is about 6 $\Omega \cdot$ cm higher than that of the haemolysis and resealing medium. This was to be expected, since the cells still contained some haemoglobin which would act to increase the resistance.

Table III shows the resistivity values determined for ghost cells which were obtained by electrical haemolysis in a hypotonic sodium phosphate-buffered KCl solution (225 mosM, $\rho_1 = 80$

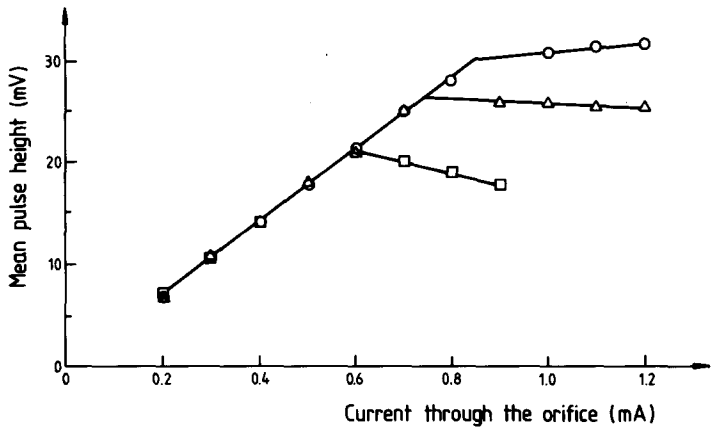

Fig. 4. The effect of increasing resistivity of the suspension medium on the pulse height of size distributions of human red blood cell ghosts measured as a function of the current through the orifice of a particle volume analyser. The different resistivities were achieved by adding isotonic sucrose solution to an isotonic sodium phosphate-buffered KCl solution. Resistivities and final sucrose concentration: O——O, 63.4 $\Omega \cdot$cm, 0 mM; △——△, 81.0 $\Omega \cdot$cm, 50 mM; □——□, 95.9 $\Omega \cdot$cm, 100 mM. Before electrical breakdown, for a given current the mean pulse heights of the size distributions are independent of the resistivity of the suspension medium. This is because the analyser uses a 'current-sensing' amplifier. After electrical breakdown the mean pulse heights depend on the resistivity of the medium. If the cell interior is more conductive than the suspension medium (△, □), the mean pulse height decreases with increasing current leading to a negative slope of the second straight line.

TABLE II

INTRACELLULAR RESISTIVITY OF HUMAN RED BLOOD CELL GHOSTS CALCULATED ACCORDING TO EQN. 18

The ratios of the slopes were obtained from measurements of the mean pulse height of a ghost cell population versus the orifice current. The different resistivities were achieved by adding isotonic sucrose solution to an isotonic sodium phosphate-buffered KCl solution. The shape factor was 1.5.

Sucrose concn. (mM)	Resistivity of the medium, ρ_1 ($\Omega \cdot$cm)	Ratio of slopes, s	Intracellular resistivity, ρ_2 ($\Omega \cdot$cm)
0	63.0	0.070	70.1
15	65.6	0.037	69.4
20	67.3	0.018	69.2
25	68.4	0.007	69.1
30	70.0	0.012	71.3
35	71.3	−0.003	71.3
40	72.8	−0.031	69.5
45	73.9	−0.063	67.3
50	75.5	−0.085	66.6

$\Omega \cdot$ cm). The shape factor was assumed to be 1.09, since the ghost cells had the same biconcave shape as intact erythrocytes. In this case, the calculated internal resistivity was also independent of the external conductivity. With 71 $\Omega \cdot$ cm, the internal resistivity value was, however, about 10 $\Omega \cdot$ cm lower than the resistivity value of the entrapped solution (80 $\Omega \cdot$ cm). The reason for this is that, as in previous examples, the electrical breakdown measurements were carried out in isotonic solutions with different conductivities. Since ghost cells behave like osmometers, there is an efflux of water, coupled with a reduction in volume, when the resealed cells are transferred to isotonic solutions. The volume reduction causes the entrapped ions to be concentrated and the conductivity to be correspondingly increased (i.e. the resistance is reduced). Measurements of this kind may well be of interest in the future, because they are suitable for testing the quality of ghost preparations (leakiness, etc.), (see Bodemann and Passow [34]).

TABLE III

INTRACELLULAR RESISTIVITY OF HUMAN RED BLOOD CELL GHOSTS CALCULATED ACCORDING TO EQN. 18

The ratio of the slopes were obtained from measurements of the mean pulse height of a ghost cell population versus the orifice current. The different resistivities were achieved by adding isotonic sucrose solution to an isotonic sodium phosphate-buffered KCl solution. In contrast to the measurements shown in Table II, here the measurements were performed with ghost cells of biconcave shape (see Methods). The intracellular resistivity is therefore calculated using a shape factor of 1.09.

Sucrose concn. (mM)	Resistivity of the medium, ρ_1 ($\Omega \cdot$cm)	Ratio of slopes, s	Intracellular resistivity, ρ_2 ($\Omega \cdot$cm)
0	60.7	0.128	70.4
20	66.0	0.078	72.0
40	71.3	0.002	71.3
60	78.3	−0.120	69.2

Discussion

The results reported here demonstrate that the internal conductivity and its changes can be accurately measured by means of a particle size analyser. In principle, it is sufficient to determine the size distribution of a given cell population at two different current values before and after breakdown at a single conductivity value of the external solution. The results show that the accuracy of the measurement is so high that it is possible to determine the ratio of the slopes of the signal vs. current curves from the two sets of measurements before and after breakdown. Given the short exposure times of the cells in the orifice at room temperature (pulse duration about 20 μs), the beakdown voltage of most cells is about 1 V and varies little with the composition of the medium. Therefore, the current value leading to electrical breakdown of the membrane can be immediately calculated with the aid of the integrated Laplace equation and Ohm's law in order to measure two distributions before and two after breakdown. The radius of the cell, which must be known for the calculation of the critical field strength on the basis of the Laplace equation, is determined under the microscope. Likewise, the shape factor of the cells is also determined under the microscope by geometrical measurement of the axial ratio of the cells under investigation. Given the value for the shape factor and the resistivity of the solution, it is then possible to calculate the intracellular resistivity on the basis of Eqn. 18.

This procedure can be automated relatively easily with the aid of a microprocessor, so that a fast and reliable (i.e. precise) method of measuring ρ_2 is obtained. With the automated process, a further simplification of the procedure can be achieved by measuring and analysing only those signals for the mean volume, rather than determining the entire size distribution for each of the four values of the current intensity (see Figs. 1 and 4).

Difficulties in analysing the data may be encountered when determining the intracellular conductivity of cells in a heterogeneous cell population with different dielectric breakdown voltages [35]. In this case, measurements have to be carried out with the aid of a single particle analyser [17,18] which enables the signal versus current curves before and after breakdown to be measured in individual cells. Finally, we would like point out that the principle of this technique is very similar to the impedance method for the determination of intracellular conductivities [32]. In the case of the impedance method, the internal conductivity is measured at high frequencies (about 100 MHz). At these high frequencies the cell membrane presents only a very low impedance although it acts as an insulator at low frequencies. In the procedure described here, dielectric breakdown causes the membrane to be converted to a low-impedance state.

The intracellular conductivity of a cell and its change (e.g. during growth or under pathological conditions) may be of more interest in the future when more information on different cell species has been accumulated with the aid of this technique.

Acknowledgements

We would like to thank Dr. W.M. Arnold for reading the manuscript, Mr. Buers for expert technical assistance and Miss Hermanns for typewriting. A grant of the Deutsche Forschungsgemeinschaft (Sonderforschungsbereich) to U.Z. for part of this work is appreciated.

References

1 Zimmermann, U., Schultz, J. and Pilwat, G. (1973) Biophys. J. 13, 1005–1013
2 Zimmermann, U., Pilwat, G., Beckers, F. and Riemann, F. (1976) Bioelectrochem. Bioenerg. 3, 58–83
3 Zimmermann, U., Vienken, J. and Pilwat, G. (1980) Bioelectrochem. Bioenerg. 7, 553–574
4 Zimmermann, U., Scheurich, P., Pilwat, G. and Benz, R. (1981) Angew. Chem. 93, 332–351, Int. Edn. 20, 325–344
5 Zimmermann, U. (1982) Biochim. Biophys. Acta 694, 227–277
6 Benz, R., Beckers, F. and Zimmermann, U. (1979) J. Membrane Biol. 48, 181–204
7 Abidor, I.G., Arakelyau, V., Chernomordik, L., Chismadzhev, Y., Pastushenko, V. and Tarasevich, M. (1979) Bioelectrochem. Bioenerg. 6, 37–62
8 Benz, R. and Zimmermann, U. (1980) Biochim. Biophys. Acta 597, 637–642
9 Dimitrov, D.S. (1984) J. Membrane Biol. 78, 53–60
10 Dimitrov, D.S. and Jain, R.K. (1984) Biochim. Biophys. Acta 779, 437–468
11 Zimmermann, U. and Vienken, J. (1982) J. Membrane Biol. 67, 165–182
12 Zimmermann, U. and Vienken, J. (1984) in Cell Fusion, Gene Transfer and Transformation (Beers, R.F. and Bassett, E.G., eds.), pp. 171–187, Raven Press, New York
13 Zimmermann, U., Vienken, J., Pilwat, G. and Arnold, W.M. (1984) in Cell Fusion (Evered, D. and Whelan, J., eds.), pp. 60–85, Pitman Books, London
14 Zimmermann, U., Vienken, J. and Pilwat, G. (1984) in Investigative Microtechniques in Medicine and Biology (Chayen, D. and Bitensky, J., eds.), pp. 89–167,Marcel Dekker, New York
15 Arnold, W.M. and Zimmermann, U. (1984) in Biological Membranes (Chapman, D., ed.), Vol. 5, pp. 389–454, Academic Press, London
16 Zimmermann, U., Büchner, K.H. and Arnold, W.M. (1984) in Charge and Field Effects (Allen, M.G. and Usherwood, P.N.R, eds.), pp. 293–318, Abacus Press, Tunbridge Wells
17 Zimmermann, U., Pilwat, G. and Groves, M.R. (1978) Deutsche Patentanmeldung P 28 28 232.8, US-Patent 42 20 916, Sept. 1980
18 Zimmermann, U., Groves, M., Schnabl, H. and Pilwat, G. (1980) J. Membrane Biol. 52, 37–50
19 Akeson, S.P. and Mel, H.C. (1983) Biophys. J. 44, 397–403
20 Akeson, S.P. and Mel, H.C. (1982) Biochim. Biophys. Acta 718, 201–211
21 Velick, S. and Gorin, M. (1940) J. Gen. Physiol. 23, 753–771
22 Hurley, J. (1970) Biophys. J. 10, 74–79
23 Grover, N.B., Naaman, J., Ben Sasson, S. and Doljanski, F. (1969) Biophys. J. 9, 1398–1414
24 Kachel, V. (1979) in Flow Cytometry and Sorting (Melamed, M.R., Mullaney, P.F. and Mendelsohn, M.L., eds.), pp. 61–104, Wiley, New York
25 Kachel, V. (1982) in Cell Analysis (Catsimpoolas, N., ed.), Vol. 1, pp. 195–331, Plenum Press, New York
26 Jeltsch, E. and Zimmermann, U. (1979) Bioelectrochem. Bioenerg. 6, 349–384
27 Haest, C.W.M., Fischer, T.M., Plasa, G. and Deuticke, B. (1980) Blood Cells 6, 539–553
28 Zimmermann, U., Pilwat, G., Holzapfel, C. and Rosenheck, K. (1976) J. Membrane Biol. 30, 135–152

29 Kinosita, K. and Tsong, T.Y. (1979) Biochim. Biophys. Acta 554, 479–497
30 Zimmermann, U., Pilwat, G. and Riemann, F. (1974) Biophys. J. 14, 881–899
31 Kachel, V. (1976) J. Histochem. Cytochem. 24, 211–230
32 Pauly, H. and Schwan, H.P. (1966) Biophys. J. 6, 621–639
33 Saleemuddin, M., Zimmermann, U. and Schneeweiss, F. (1977) Z. Naturforsch. 32c, 627–631
34 Bodemann, H. and Passow, H. (1972) J. Membrane Biol. 8, 1–26
35 Zimmermann, U., Riemann, F. and Pilwat, G. (1976) Biochim. Biophys. Acta 436, 460–474